Chapter 2
Law of Asymptotic Linearity

2.1 Definition and Genesis

In this chapter, a new law is proposed that, to the best of my knowledge, has not yet been discussed as such in the literature. According to the law, all subjective magnitudes grow linearly with the intensities of the stimuli that evoke them near their thresholds of detectability. The relationship was first discovered during auditory measurements concerning Stevens' Power Law and is described here initially for loudness, then generalized. When sufficiently small stimulus magnitudes were included, the resulting loudness curves deviated from the power law and, on double-logarithmic coordinates, bent downward, becoming gradually steeper. A typical example is shown in Fig. 2.1 where loudness magnitudes of a 1,000-Hz tone are plotted over sound-intensity abscissas expressed in dB (Hellman and Zwislocki, 1963). The solid curve has been determined by the method of magnitude estimation based on two reference standards, as described in the preceding chapter (Hellman and Zwislocki, 1961). The slanted crosses show averages of 12 studies computed by Robinson (1957), in which various methods were used. Filled circles indicate the data of Stevens (1956) obtained by magnitude estimation with the reference standards chosen by the observers themselves; open symbols and filled triangles, the data of Scharf and Stevens (1961) obtained by magnitude estimation with a designated reference standard and by halving and doubling; the vertical crosses, the data determined by Feldtkeller et al. (1959) with the help of the same method. The excellent agreement between the various sets of data and the curve suggests that the curve accurately represents the loudness of a 1,000-Hz tone as a function of its intensity. Of particular interest is the asymptotic convergence of the curve on a linear relationship between loudness and sound intensity near the threshold of audibility, as indicated by the straight line having the coordinates of 0.01 at zero SL (threshold of audibility) and 1 at 20 dB.

The linear relationship between the loudness of a 1,000-Hz tone and its sound intensity near the threshold of audibility may have been first noticed by Zwicker and Feldtkeller (1956). Their graphical representation of the relationship is shown

J.J. Zwislocki, *Sensory Neuroscience: Four Laws of Psychophysics,*
DOI: 10.1007/978-0-387-84849-5_2,
© Springer Science+Business Media LLC 2009

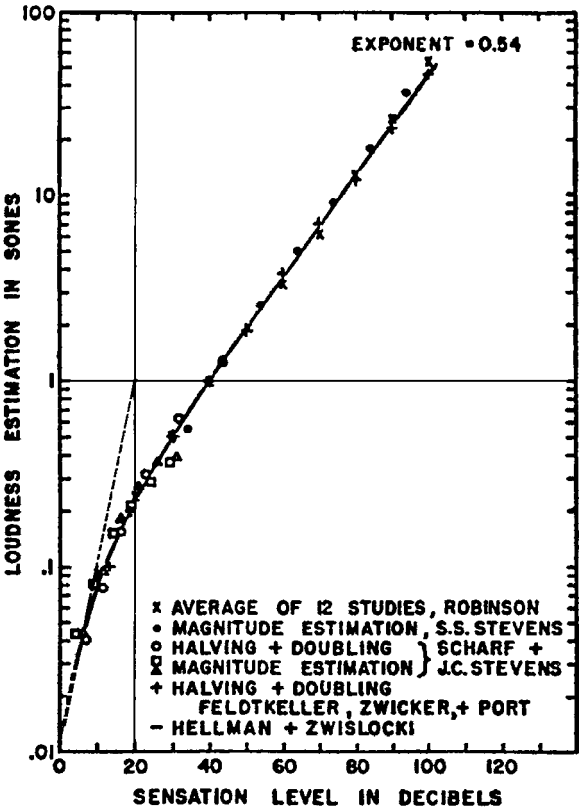

Fig. 2.1 A typical binaural loudness function (solid line) determined with two reference standards and compared to the results of five other studies performed with different methods. The intermittent straight line shows a linear relationship between loudness and sound intensity. Modified from Hellman and Zwislocki (1963), reproduced with permission from the American Institute of Physics

in Fig. 2.2, where it is denoted symbolically as $N \sim p^2$ with N standing for loudness and p for sound pressure. Of course, sound intensity is directly proportional to the square of the latter.

Is the linear relationship between loudness and sound intensity near the threshold of audibility an exclusive property of the 1,000-Hz tone, or does it extend to other sound frequencies? An experiment in which loudness was determined by the method of numerical magnitude balance at 100 Hz, 250 Hz and 1,000 Hz proved the latter to be true (Hellman and Zwislocki, 1968). As an example, geometric-mean data obtained on nine observers at 100 Hz are shown in Fig. 2.3 on double-logarithmic coordinates. The filled circles resulted from magnitude estimation, the crosses, from magnitude production. The solid line joins the geometric means of their interpolated values. The straight line with the coordinates 40 dB, 0.001 dB and 60 dB, 0.1 indicates a linear relationship between loudness and sound pressure squared. It parallels the mean loudness curve at its lowest values. Interestingly, the

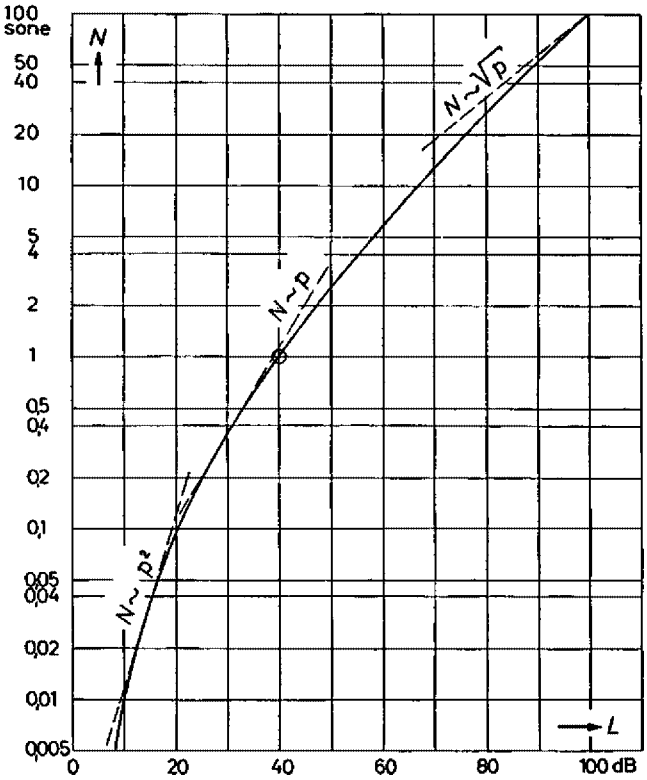

Fig. 2.2 Loudness as a function of SPL (L) determined on eight listeners by the method of halving and doubling. Loudness is indicated by N and sound pressure by p. The intermittent tangent lines indicate the slope of the function at three locations. The lowest parallels a linear relationship between loudness and sound pressure squared. Reproduced from Zwicker and Feldtkeller (1956) with permission from S. Hirzel Verlag

curve becomes somewhat steeper above these values before flattening. Geometric-mean curves obtained at all three sound frequencies are shown in Fig. 2.4. Slanted crosses indicate the respective thresholds of detectability. As a reference, straight lines with a slope of one with respect to the sound pressure squared and originating at 0 dB, 20 dB and 40 dB, respectively, are included in the graph. They are paralleled by all the loudness functions, irrespective of sound frequency. Consequently, the linearity of loudness functions near the threshold of detectability appears to hold for all sound frequencies at and below 1,000 Hz.

The slope constancy of the near-threshold loudness curves between 100 Hz and 1,000 Hz can be verified by direct inter-frequency loudness matching. Many studies were performed in which the loudness magnitudes of tones at various sound frequencies were matched to those at 1,000 Hz. The procedure consisted essentially of finding sound intensity levels referred to those at 1,000 Hz, which produced the same loudness magnitudes. Data obtained in this way at 100 Hz and 250 Hz in some

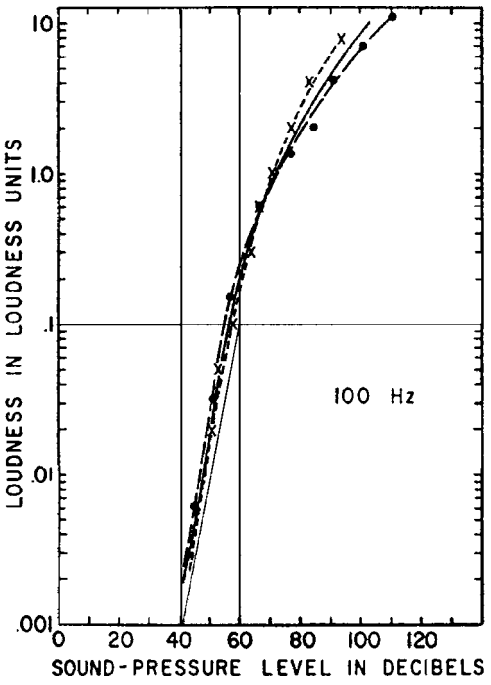

Fig. 2.3 Loudness of a 100-Hz tone determined by magnitude balance as a function of SPL. Filled circles indicate geometric means of data obtained by absolute magnitude estimation, crosses, those obtained by absolute magnitude production, the solid curve indicates their interpolated geometric means. The solid straight line indicates a linear relationship between loudness and sound intensity. Modified from Hellman and Zwislocki (1968), reproduced with permission from the American Institute of Physics

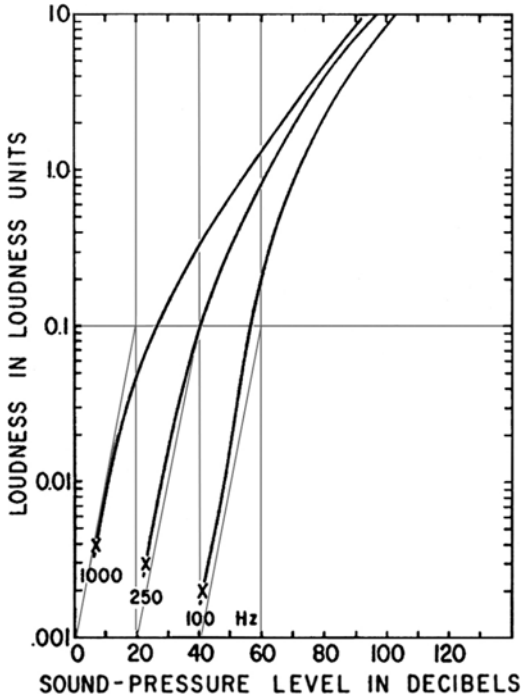

Fig. 2.4 Loudness functions determined at three sound frequencies, 100, 250 and 1,000 Hz, by numerical magnitude balance. Crosses indicate the corresponding thresholds of audibility, and the slanted straight lines, a linear relationship between loudness and sound intensity. Modified from Hellman and Zwislocki (1968), reproduced with permission from the American Institute of Physics

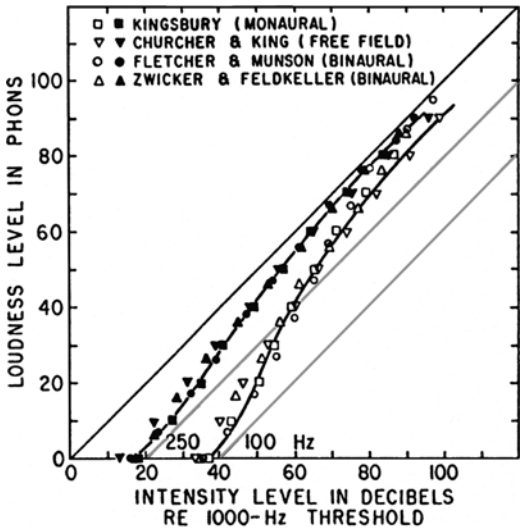

Fig. 2.5 Loudness-level curves at 100 and 250 Hz referred to the loudness at 1,000 Hz and obtained by horizontal cuts through the family of curves of Fig. 2.4. The various symbols indicate the results of corresponding direct loudness matches obtained in several studies. The slanted lines parallel the reference diagonal line and show that, at near-threshold intensities, all loudness functions are parallel to each other

classical studies spanning a period of 40 years are shown in Fig. 2.5. They are compared to the results derived from Fig. 2.4 by sectioning horizontally the family of the curves of that figure (Hellman and Zwislocki, 1968). Note that, at near threshold levels, the curves with all the data points clustered around them parallel the diagonal line indicating the reference slope at 1,000 Hz. Similar, although less detailed, results were obtained at higher sound frequencies (e.g. Scharf, 1978). The conclusion seems warranted that, at least for pure tones, loudness is related linearly to sound intensity near the threshold of audibility.

What happens when the test tone is not presented in quiet but in the presence of masking noise that increases the slope of the loudness function, or the slope is increased by an auditory defect?

Results of a masking experiment performed on a 1,000-Hz tone are shown graphically in Fig. 2.6 (Hellman and Zwislocki, 1964). The masking stimulus consisted of an octave band of random noise centered on the test-tone frequency. It was presented at two intensity levels, so as to produce threshold shifts of 40 dB and 60 dB, respectively. The loudness levels of the partially masked tone were measured directly by comparing them to the loudness of the same tone in the absence of the masking noise. The corresponding results are shown in Fig. 2.6 by the filled circles. The abscissa axis refers to the threshold of audibility in the masked ear in the absence of the masker, the ordinate axis, to the threshold of audibility in the unmasked ear. The diagonal line corresponds to the loudness level of the unmasked tone. The curves indicate loudness levels derived from loudness measurements by the method of magnitude production. The results of these measurements agreed better with direct loudness matches than did the results of numerical loudness balance. The straight lines drawn through the threshold points parallel to the diagonal line are linearly related to sound intensity. The loudness-level curves appear to converge on them near the thresholds but the paucity of the data points leaves some uncertainty in this respect.

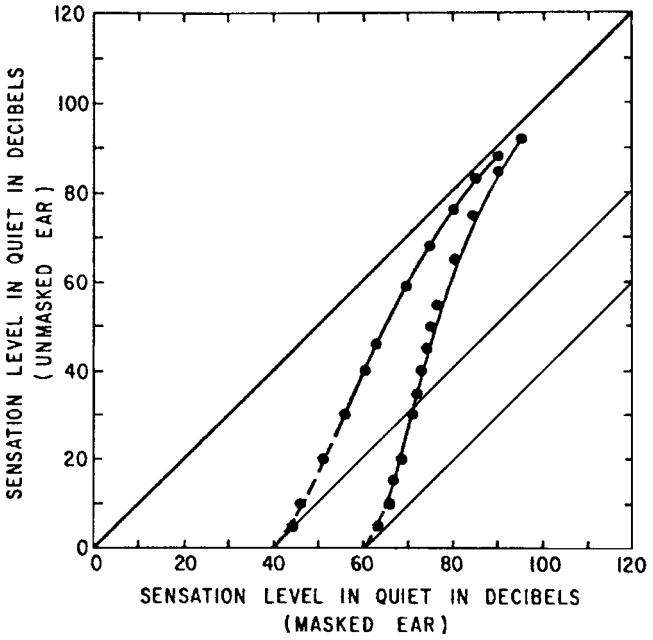

Fig. 2.6 Loudness-level curves obtained by comparing the loudness of a partially masked 1,000-Hz tone to that of an unmasked 1,000-Hz tone at two masking levels. Corresponding data derived from absolute magnitude production are indicated by filled circles. Slanted lines parallel to the diagonal indicate that masking did not alter the slope of the loudness functions near the threshold of audibility. Modified from Hellman and Zwislocki (1964), reproduced with permission from the American Institute of Physics

More convincing results were presented by B.C.J. Moore (2004) who performed experiments on four observers with sensorineural hearing loss, most likely of cochlear origin. In three observers, the hearing loss was bilaterally asymmetrical, in the fourth, it was symmetrical but affected exclusively sound frequencies above 1,000 Hz. The experiments aimed specifically at loudness growth near the threshold of audibility. They consisted of both threshold measurements and heterofrequency loudness matching. For the latter, a frequency associated with a substantial hearing loss was paired with a frequency associated with a minimal hearing loss. The experiments were performed by means of modern adaptive procedures with respect to both threshold measurements and loudness matching, assuring maximal accuracy of the results. In all four observers, when the threshold was approached, loudness grew at a rate independent of hearing loss and the slope of the loudness curve at higher sensation levels. Two examples of Moore's graphs are reproduced in Figs. 2.7 and 2.8. In both, the sensation levels corresponding to the greater hearing loss are given by the abscissas, those corresponding to the smaller hearing loss, by the ordinates. The dashed diagonal line indicates parallel loudness growth in both instances. Clearly, at near-threshold levels, all the experimental points converge on the diagonal line, indicating the same rate of loudness growth independent of hearing loss. Since the latter

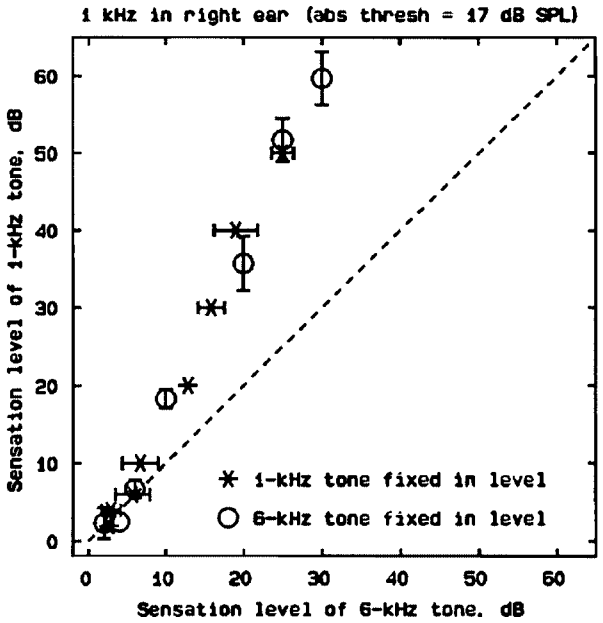

Fig. 2.7 Sensation level of a 1-kHz tone in the presence of a small hearing loss as a function of the sensation level of a 6 kHz tone in the presence of a greater hearing loss, both tones presented to the same ear at equal loudness. The slope of the resulting implied curve converges on the slope of the diagonal, indicating that the difference in hearing loss did not affect the slope of the loudness function near the threshold of audibility. Reproduced from Moore (2004) with permission from the American Institute of Physics

was negligible in one ear, the growth had to be linearly related to sound intensity, as was shown in older experiments (e.g. Hellman and Zwislocki, 1963).

The experimental evidence cited above is consistent throughout with a constant loudness growth, linearly related to sound intensity, at near threshold sensation levels, independent of sound frequency, hearing loss, or the rate of loudness growth at higher levels. The putative biophysical process responsible for the constancy is described in the following section. It is directly associated with the basic tenants of the theory of signal detectability (Green and Swets, 1966) and, in this way, provides a bridge between this theory and loudness scaling.

2.2 Underlying Biophysical Process

In all systems that are not at a temperature of absolute zero, heat is associated with molecular motion. Sensory receptors are no exception, and molecular noise was included explicitly or implicitly for many decades in the analyses of the detection of sensory signals. For example, Miller (1947) suggested that the masking effect

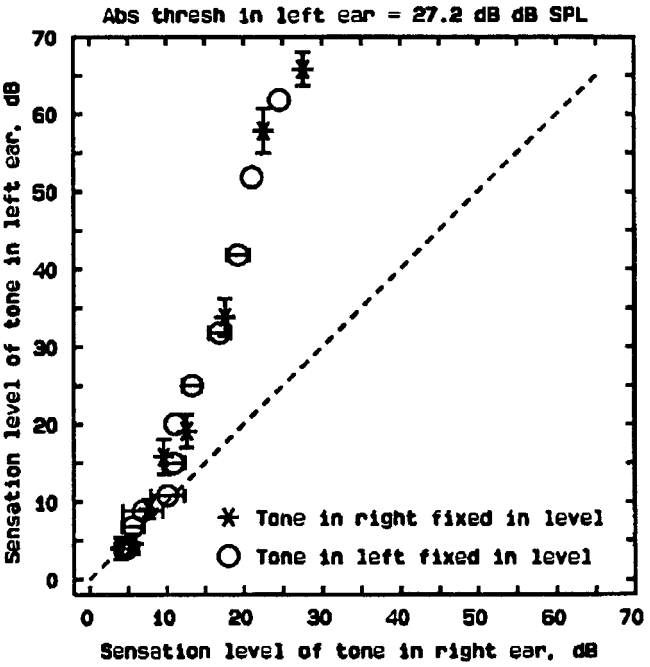

Fig. 2.8 Similar to Fig. 2.7, except that the tones were presented to different ears. Reproduced from Moore (2004) with permission from the American Institute of Physics

exerted by an extrinsic auditory noise on a pure-tone signal departed from a constant signal-to-noise ratio near the absolute threshold as a result of intrinsic noise. In vision, an analogous phenomenon is attributed to internal noise called "dark light" (e.g. Barlow, 1972). Later on, the internal noise became a fundamental postulate of the theory of signal detectability, and sensory thresholds became defined as percentages of successful discriminations between signal-plus-noise and noise-alone events (e.g. Green and Swets, 1966).

Internal noise is difficult to detect in the electrical potentials of sensory receptors because of the interfering noise of recording electrodes but its effect is clearly visible in the spontaneous activity of neurons innervating the receptors, where it appears in a digital form. The activity has been particularly thoroughly studied in afferent neurons of the auditory nerve. An example of a corresponding input/output characteristic of an auditory neuron is shown in Fig. 2.9 on double-logarithmic coordinates. The crosses indicate recorded firing rates and the star the average spontaneous activity according to Kiang (1968). The solid line through the crosses shows a theoretical approximation of the data with the inclusion of the spontaneous activity, the intermittent line, after its subtraction (Zwislocki, 1974). The lowest straight line indicates an asymptote of the intermittent line with the slope of one, in other words, a linear relationship to sound intensity.

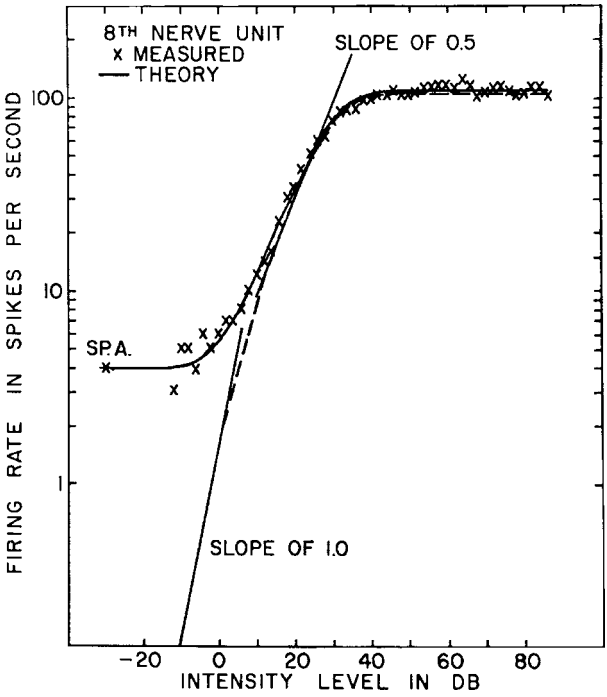

Fig. 2.9 A typical intensity characteristic of an auditory-nerve fiber. The crosses show the empirical data, the curves, their theoretical approximations. The spontaneous activity (SP. A.) is indicated by the star. The intermittent line shows the total neuronal firing rate less the spontaneous activity. It converges at low intensities on a tangent linearly related to sound intensity. Reproduced from Zwislocki (1974), with permission from copyright holder

The asymptote has been obtained analytically on the assumption that the spontaneous activity expresses the internal noise intensity that is added to the signal intensity (Zwislocki, 1973, 1974). Accordingly, the total stimulus intensity is

$$S_{\mathrm{T}} = (S + N_{\mathrm{I}}) \tag{2.1}$$

where S means the signal intensity and N_{I}, the internal noise intensity. At medium signal levels, the firing rate follows a slope of 0.5, in other words, the stimulus amplitude. This can be expressed mathematically by taking the square root of the expression in the parenthesis, so that

$$R(S_{\mathrm{T}}) = A(S + N_{\mathrm{I}})^{0.5} \tag{2.2}$$

where $R(S_{\mathrm{T}})$ means the total firing rate and A is a dimensional constant. The latter equation can be written in the form

$$R(S_{\mathrm{T}}) = R_{\mathrm{o}}(1 + S/N_{\mathrm{I}})^{0.5} \tag{2.3}$$

with $R_o = AN_I^{0.5}$ standing for the spontaneous activity. For $S/N_I \ll 1$, Eq. 2.3 can be approximated by the first two terms of its Taylor expansion, leading to

$$R(S_T) \cong R_o(1 + 0.5\ S/N_I) \tag{2.4}$$

By subtracting R_o, we obtain the driven neural firing rate,

$$R_D(S) \cong 0.5\ R_o S/N_I \tag{2.5}$$

Note that it is directly proportional to the stimulus intensity, not amplitude. Equally important, the direct proportionality is independent of the exponent, 0.5 and would not be affected if the exponent were different or even the exponential function replaced by another ascending, monotonic function. This is so because of the properties of the Taylor expansion. As a consequence, all the sensory neurons exhibiting spontaneous activity should have near-threshold firing rates that are directly proportional to the stimulus intensity.

What happens when there is no spontaneous neural activity or the activity is so small that it cannot be used as a measure of the internal noise. Under such conditions, we can write for the receptor potential with the continuous use of the power-function approximation

$$E = B(E_s + E_I)^{\beta}. \tag{2.6}$$

where E means the total receptor potential, E_S and E_I, the receptor potentials generated by the signal and internal noise, respectively, β, a generalized power exponent, and B, a dimensional constant. For the neural firing rate, we can write on the assumption that it is linearly related to the receptor potential (e.g. Fuortes, 1971)

$$R(S_T) = C(E_S + E_I)^{\beta} - T \tag{2.7}$$

where $R(S_T)$ signifies the total firing rate, C, a dimensional constant and T, the firing threshold. When $E_S \ll E_I$, we can again use the Taylor approximation, so that

$$\begin{aligned} R(S_T &= CE_I^{\beta}(1 + \beta E_S/E_I) - T \\ T &\leqslant CE_I^{\beta} \end{aligned} \tag{2.8}$$

or

$$R(S_T) = C\beta E_I^{\beta-1} E_S + (CE_I^{\beta} - T) \tag{2.9}$$

Accordingly, the driven firing rate remains linearly related to the signal intensity.

The above analysis shows that, for signal intensities smaller than the intensity of the internal noise, the neuronal firing rate must be approximately linearly related to the intensity of the stimulating signal. But does such linearity hold for psychological responses that are not controlled by single neurons but, rather, aggregates of neurons? One necessary condition is satisfied – the sum of linear functions is a linear function. More specifically, if the firing rates of neurons in an aggregate follow linear functions, the same must be true for the whole aggregate.

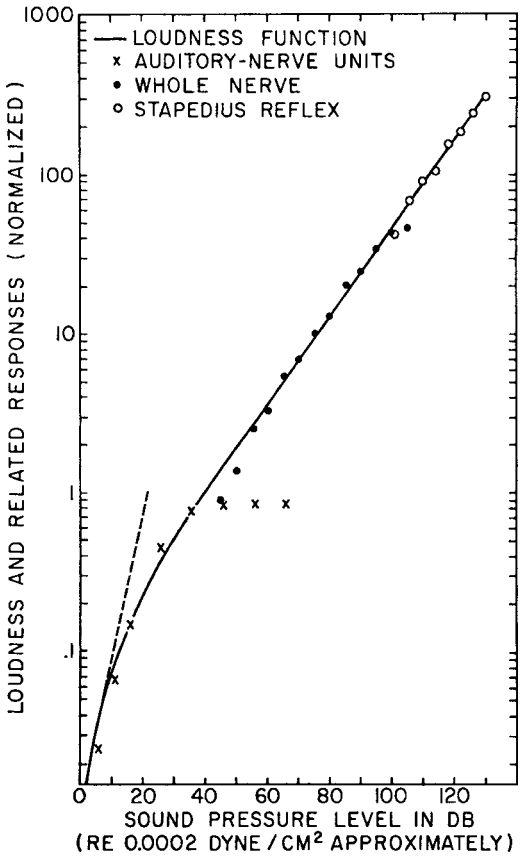

Fig. 2.10 A typical loudness function (Hellman and Zwislocki, 1961) is compared to a normalized driven firing rate of an auditory-nerve fiber (crosses; Zwislocki, 1973), integrated response of the auditory nerve (filled circles; Teas et al., 1962) and the strength of the stapedius-muscle reflex (unfilled circles; Zwislocki and Shepherd, 1972). All the characteristics tend to parallel each other. The loudness function and driven neural activity converge on a linear relationship to sound intensity at low sound intensities (intermittent straight line). Modified from Zwislocki (1974), with permission from copyright holder

The above analysis has been applied to sensory receptors and peripheral neurons but psychological responses involve higher stages of the nervous system. Does the linearity hold there for small signals? Probably yes, for the same reasons that it holds for the periphery, but we cannot be sure. Direct empirical evidence is necessary. Several examples of such evidence have been given for the auditory system in the first section. A more explicit one is shown graphically in Fig. 2.10. The loudness curve of Fig. 2.1 (solid line) is compared to the normalized driven firing rates of a single neuron in the auditory nerve (crosses) as well as to the electrical whole-nerve response (filled circles) and the contraction strength of the stapedius muscle, as reflected in the acoustic-impedance change at the tympanic membrane (unfilled circles) (Zwislocki, 1974, 2002). Note that all the characteristics tend to parallel each other, except for the saturation section of the single-neuron characteristic. Note in particular that the single-neuron characteristic parallels the loudness curve at low signal levels. Additional evidence can be found in the next section concerning the generality of the asymptotic-linearity law.

2.3 Generality

Because of the postulated linear summation evident in Fig. 2.10, the analysis concerning single neurons can be extended to neuronal aggregates and psychophysical experiments. Auditory masking experiments in which a pure tone is masked by random noise are of particular interest. The analysis can be applied to them by simply adding the external noise intensity, N_{M}, to the internal noise intensity, $\mathrm{N_I}$, producing the total noise intensity, $N_{\mathrm{T}} = N_{\mathrm{I}} + N_{\mathrm{M}}$. One caveat must be observed, however. Only the portion of the extrinsic noise intensity that contributes to the masking effect should be included. Frequency bands sufficiently removed from the test-tone frequency not having such an effect must be excluded. Under these conditions, the total loudness of the tone and noise together obeys the equation (Zwislocki, 1965)

$$L_{\mathrm{T}} = a(S + N_{\mathrm{I}} + N_{\mathrm{M}})^{\theta} \tag{2.10}$$

where L_{T} means the total loudness, a, a dimensional constant, and θ, a power exponent on the order of 0.3 for tone frequencies that are not very low. The equation can be rewritten in the form

$$L_{\mathrm{T}} = a(N_{\mathrm{I}} + N_{\mathrm{M}})^{\theta}\,(1 + \theta S/(N_{\mathrm{I}} + N_{\mathrm{M}}))^{\theta}. \tag{2.11}$$

and, for $S \ll (N_{\mathrm{I}} + N_{\mathrm{M}})$, approximated by

$$L_{\mathrm{T}} = a(N_{\mathrm{I}} + N_{\mathrm{M}})^{\theta}(1 + \theta S/(N_{\mathrm{I}} + N_{\mathrm{M}})) \tag{2.12}$$

For listening to the tone alone, the loudness near the threshold of detectability becomes

$$L_{\mathrm{s}} = a\theta(N_{\mathrm{I}} + N_{\mathrm{M}})^{\theta-1} S \tag{2.13}$$

and, according to the theory, should be directly proportional to the tone intensity. This is confirmed by the monaural loudness curves of Fig. 2.11 determined by the method of numerical magnitude balance in the absence ($N_{\mathrm{M}} = 0$) and the presence of masking noise at two levels, respectively. The uppermost curve was obtained in the absence of noise, the next curve, in the presence of noise that was presented intermittently in the time gaps between tone bursts and did not produce any direct masking, for the next two curves, the noise was continuous and produced partial masking of the tone bursts. At near-threshold tone intensities, all the curves approach a linear relationship to tone intensity, as is shown by the extrapolating intermittent lines. This is in agreement with the loudness-level curves of Fig. 2.6 obtained in the same experiment and having slopes independent of the masking level near the threshold of detectability. The curves of Fig. 2.11 can be approximated over their entire range by Eq. 2.10 when the loudness of the noise is subtracted (Zwislocki, 1965).

$$L = a(S + N_{\mathrm{I}} + N_{\mathrm{M}})^{\theta} - a(N_{\mathrm{I}} + N_{\mathrm{M}})^{\theta} \tag{2.14}$$

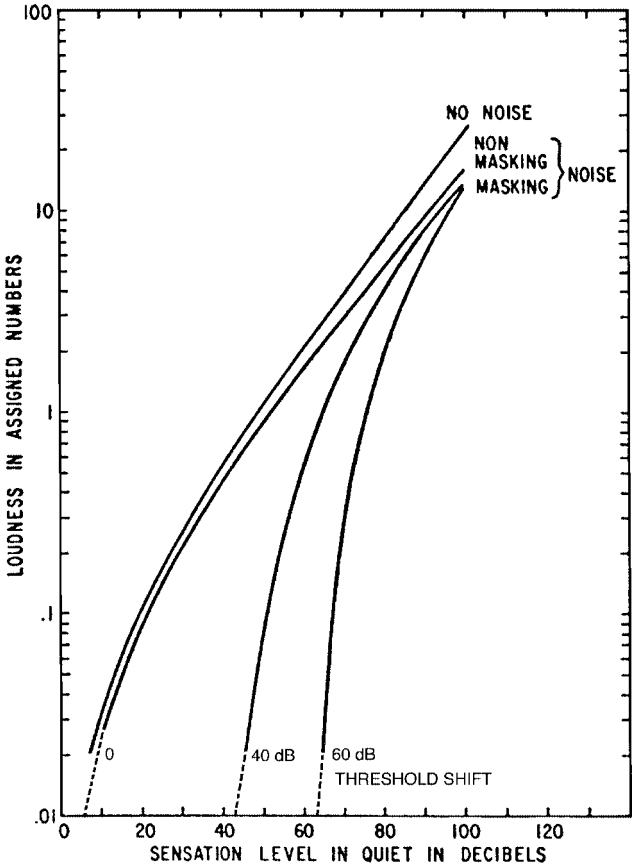

Fig. 2.11 Loudness curves at 1,000 Hz determined by numerical magnitude balance in the absence and presence of masking noise. Uppermost curve–no noise; next curve – nonmasking noise in the gaps between tone bursts; lowest two curves – masking noise at two levels presented continuously. Intermittent extrapolating lines show a linear relationship to sound intensity. Modified from Hellman and Zwislocki (1964), reproduced by permission of the American Institute of Physics

Similar subjective intensity characteristics can be obtained for the sense of touch by using vibrotactile stimuli. The similarity is only superficial, however, because the characteristics result from an entirely different mechano-receptive system, actually consisting of four systems based on four different kinds of receptors (Bolanowski et al., 1988). An example for sinusoidal vibration at a frequency of 250 Hz is shown in Fig. 2.12 with reference to sensation level (Verrillo et al., 1969). The stimulus was delivered to the thenar eminence of the right hand by a solid vibrator with a flat, circular contact surface that was pressed against the skin surface so that it produced an indentation of 0.5 mm. The surface had an area of 2.9 cm^2, and the stimuli consisted of 600 ms bursts separated by 1,400-ms time intervals. To avoid detectable transients, the stimuli were turned on and off with 10-ms ramps. The vibration

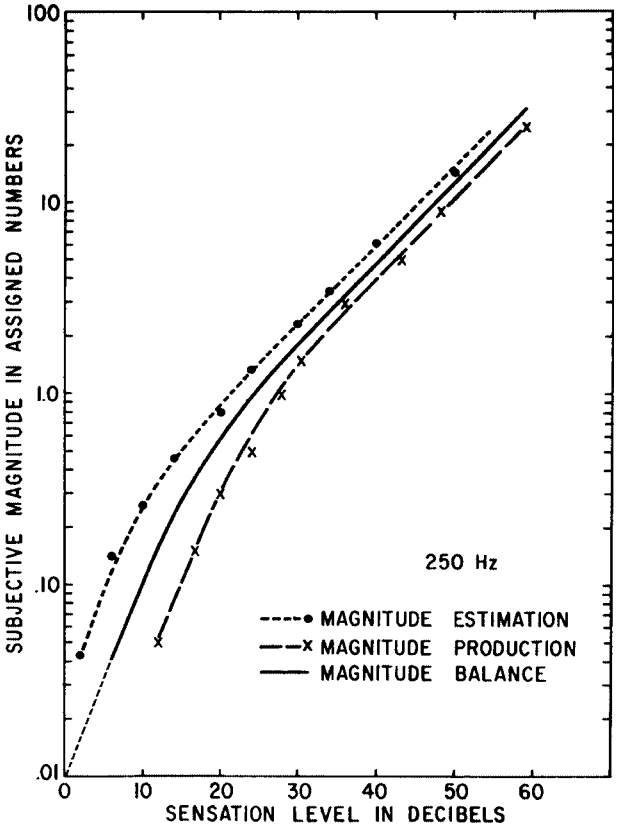

Fig. 2.12 Subjective magnitude of vibration as a function of vibration intensity. A cylindrical vibrator with a contactor area of 2.9 cm^2 was placed on the thenar eminence of the right hand and vibrated perpendicularly to the skin surface with a frequency of 250 Hz. The six observers participating in the experiment responded according to numerical magnitude balance. The resulting curve has been extrapolated downwards linearly with respect to vibration intensity. Modified from Verrillo et al. (1969), reproduced with permission from the Psychonomic Society

amplitude was measured directly with the help of an accelerometer. The subjective intensity of vibration was determined on six observers with the method of numerical magnitude balance described in Chap. 1. The filled circles of Fig. 2.12 indicate the results of magnitude estimation, the crosses, those of magnitude production. The solid line approximates their interpolated geometric means. Its extrapolation by the intermittent line obeys a linear relationship between the subjective magnitudes and the vibration amplitudes squared, proportional to intensity, in conformity with the law of asymptotic linearity.

Results obtained by the same method for several additional vibration frequencies are summarized in Fig. 2.13 by means of magnitude-balance curves. They are plotted with reference to absolute vibration amplitudes in microns rather than to sensation levels. In this way, the sensitivity differences among the various vibration

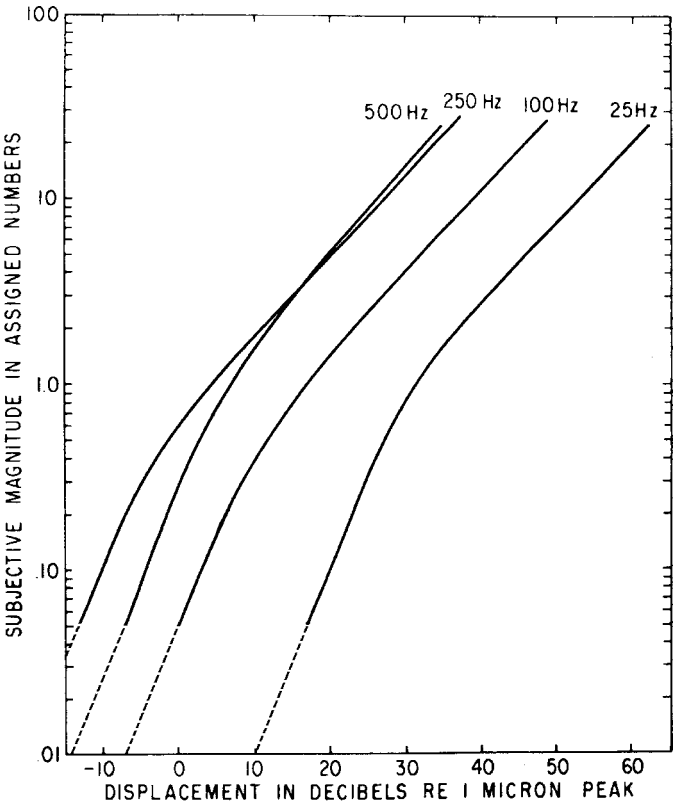

Fig. 2.13 Subjective magnitudes of vibration at four frequencies. The experimental method was the same as in Fig. 2.12. The intermittent lines extrapolate the experimental curves linearly with respect to vibration intensity. Modified from Verrillo et al. (1969), reproduced with permission from the Psychonomic Society

frequencies can be seen. Again, the extrapolating intermittent lines obey the law of asymptotic linearity with respect to vibration amplitudes squared.

The conservation of the law at all the vibration frequencies involved is of particular interest because, according to Verrillo (1966) and also Bolanowski et al. (1988), the tactile sensation at 25 Hz is mediated by different sensory receptors than that at the higher frequencies, which is mediated by Pacinian corpuscles. The preponderance of neurons ending on Pacinian corpuscles does not exhibit any spontaneous activity but the most sensitive do (Bolanowski and Zwislocki, 1984). The latter are likely the ones that determine the threshold of detectability and the shape of the subjective intensity function at near-threshold stimulus intensities. Firing-rate characteristics of one such unit are shown in Fig. 2.14 for several frequencies of vibration. Of particular interest are the curves indicating the patterns of emergence of driven firing rate from the spontaneous firing rate. They conform approximately to Eq. 2.4, thus, to the law of asymptotic linearity. A typical characteristic of a unit

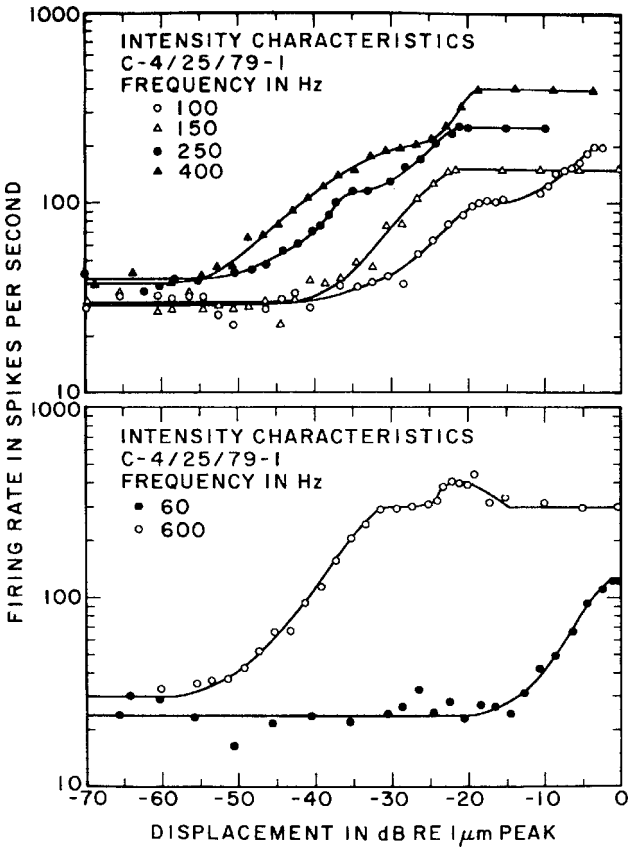

Fig. 2.14 Firing-rate characteristics of a Pacinian-corpuscle unit showing spontaneous activity. The firing rate was measured at several vibration frequencies. In the transition sections between the spontaneous and driven firing rates, the experimental curves are consistent with a linear relationship between the driven firing rate and stimulus intensity. Reproduced from Bolanowski and Zwislocki (1984), with permission from the American Physiological Society

without spontaneous activity is shown in Fig. 2.15. Its axon seems to have a high firing threshold, so that its firing pattern is not appreciably affected by the physiological noise. As a result, its action potentials tend to be synchronized with the stimulus periodicity. Such units probably control the overall response characteristics at higher vibration intensities.

Auditory and tactile receptors respond to mechanical stimuli. The input to visual receptors, the rods and cons, consists of electromagnetic waves. Does the law of asymptotic linearity still apply to vision in spite of the fundamental difference in the physical nature of the stimuli? The brightness characteristics of Figs. 2.16 and 2.17 indicate that it does (Barlow and Verrillo, 1976). The solid lines in both figures are the same and approximate the medians of absolute magnitude estimates (AMEs; Chap. 1) made by six observers at nine light intensities ranging from

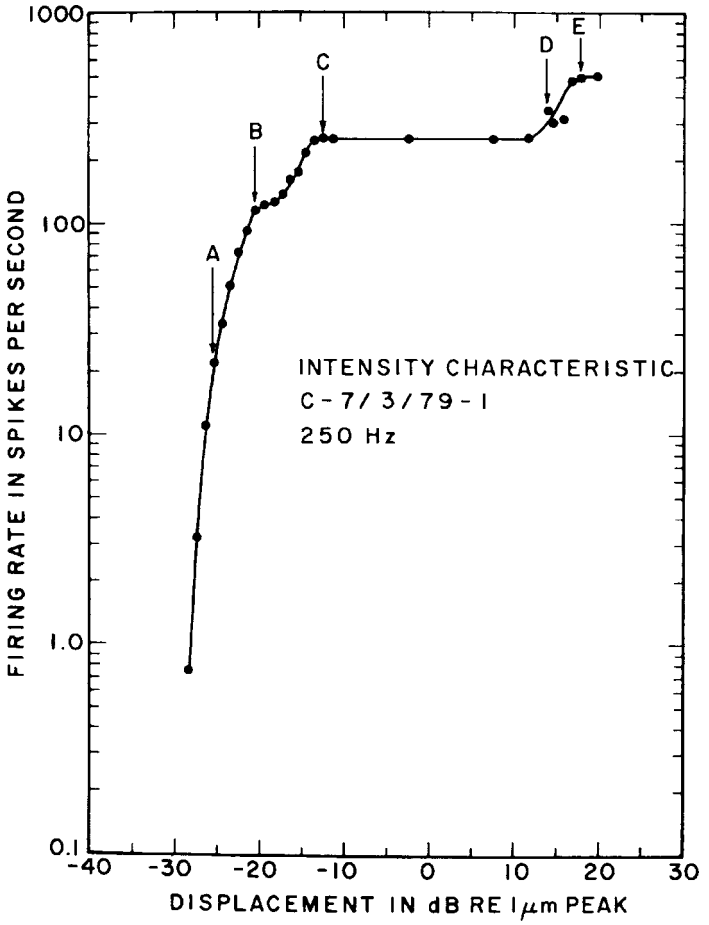

Fig. 2.15 Firing-rate characteristics of a Pacinian-corpuscle unit without spontaneous activity at 250 Hz. Reproduced from Bolanowski and Zwislocki (1984), with permission from the American Physiological Society

-9 to 0 log units ($0\,\log \cong 100\,\text{mLamberts}$) in a ganzfeld illumination. The latter was obtained by diffusing the light beam of a tungsten-filament 750 W bulb (color temperature $= 2,800\,^{\circ}\text{K}$) with half a ping-pong ball attached at the end of a blackened cone. The light intensity was controlled by means of neutral density filters. No artificial pupil was used. The observers were dark adapted before the experiment and after every light presentation that consisted of a 1-s flash. They made three brightness estimates at every intensity. The first was made for training purposes and was not included in the data averaging to minimize the response bias known to be inherent in magnitude estimation. The median brightness estimates made by the six observers are indicated in Fig. 2.16 by the crosses. The remaining symbols show the individual data obtained by taking the geometric means of two brightness estimates.

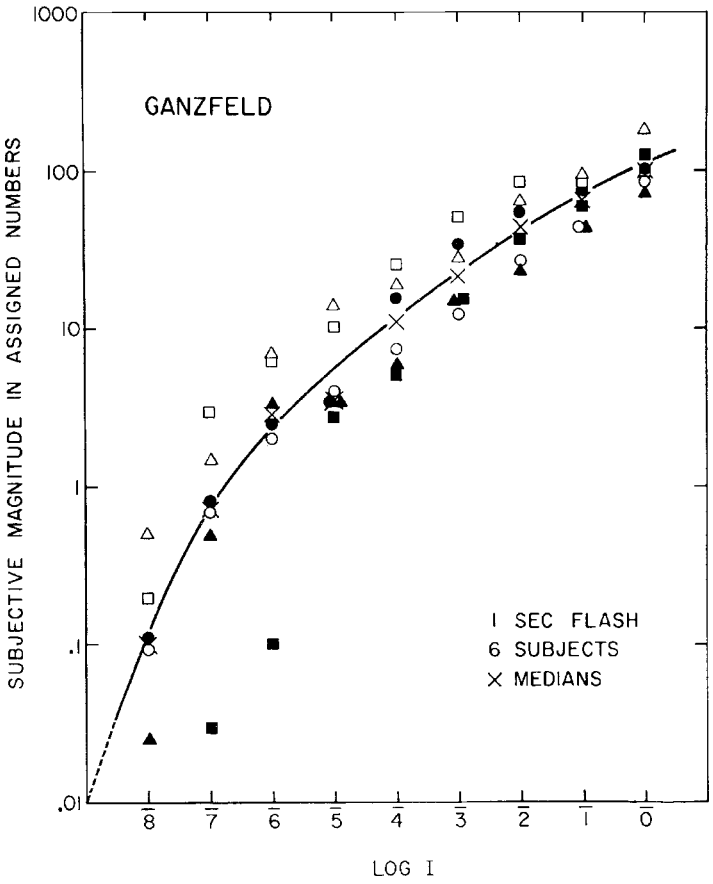

Fig. 2.16 Brightness of 1-s flashes of light produced by a 750-W tungsten-filament bulb in a ganzfeld. The brightness was measured by absolute magnitude estimation as a function of light intensity on six observers. The individual data are shown by the various symbols. The crosses indicate their medians. The solid curve is fitted to them by eye and extrapolated linearly by the intermittent line. Modified from Barlow and Verrillo (1976), with permission from Elsevier

The ganzfeld illumination was used to avoid contrast effects. To determine the effect produced by visual contrast, the light field was restricted to 2° of solid angle and presented on a black background. The median results obtained with such a field on six observers are illustrated in Fig. 2.17. In agreement with other studies, the contrast effect and the size of the illuminated field had only a small effect on brightness judgments, as indicated by the unfilled circles.

In both Figs. 2.16 and 2.17, the intermittent straight lines extrapolating the experimental data have a slope of one, indicating that the corresponding brightness functions converge on a linear relationship between the estimated brightness and light intensity. Thus, the law of asymptotic linearity applies to vision under both conditions, ganzfeld and a small target displayed on a black background.

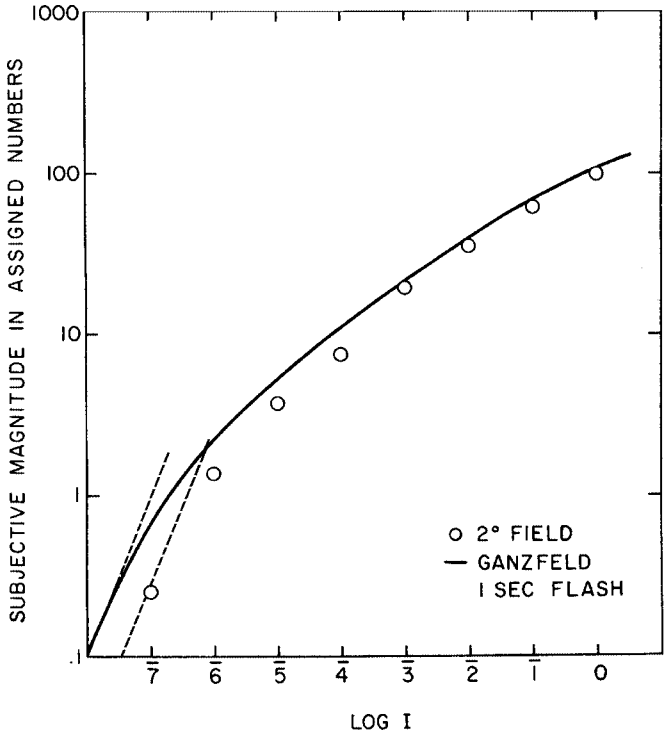

Fig. 2.17 The same as Fig. 2.16 but for a target subtending a 2° solid angle on a black background. The results, indicated by the unfilled circles, are compared to the ganzfeld results of Fig. 2.16. The intermittent lines parallel a linear function of light intensity. Modified from Barlow and Verrillo (1976), with permission from Elsevier

The results described above were obtained with dark-adapted eyes, but does asymptotic linearity hold when the eyes are light-adapted? The answer is provided by the right-hand set of data points in Fig. 2.18. They have been obtained monocularly with a circular target subtending a solid angle of 5° and displayed on a black background after the eye had been adapted for three minutes to the brightness of 106 dB re 10^{-10} Lamberts produced by illuminating a white cardboard with a flood light (J.C. Stevens and Stevens, 1963). Only the right eye was light adapted. The left eye remained dark adapted. The stimuli were presented alternately to both eyes for 2 s each, and the ten observers participating in the experiment estimated the experienced brightness magnitudes with reference to a 74-dB stimulus presented to the dark-adapted eye, to which the number 10 was assigned by the experimenter. Every stimulus was presented twice in a random order. The geometric means and the inter quartile ranges of the observers' estimates are displayed in Fig. 2.18 by means of the unfilled circles and the vertical bars, respectively. All the data points were shifted upward by a constant distance so as to bring the dark-adaptation data into coincidence with the Brill scale. They were approximated by a straight line. This

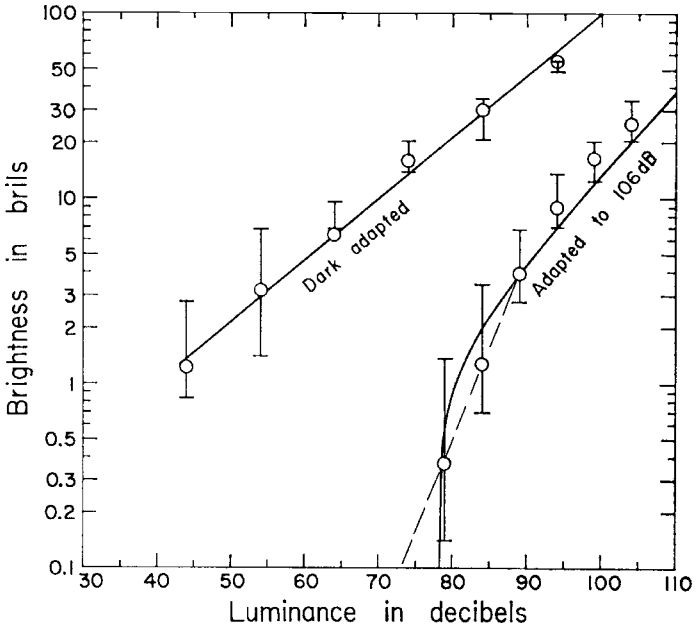

Fig. 2.18 The effect of monocular light adaptation on brightness. The right eye was adapted to 106 dB light intensity relative to 10^{-10} Lamberts (right set of data points), the left eye was dark adapted (left set of points). An illuminated target subtending a solid angle of 5° with a black surround was presented alternately to the two eyes, and ten observers estimated its brightness relative to a standard of 74 dB presented to the dark-adapted eye and called 10. The results were normalized to make the data obtained under dark adaptation coincide with the Brill scale. These data were fitted with a power function. The data obtained under light adaptation were fitted, probably erroneously, with a curve obeying Eq. 2.15. The intermittent line shows that they are linearly related to light intensity at low light intensities. The data obtained under dark adaptation do not seem to have reached sufficiently low light intensities to show the linearity effect. Modified from Stevens and Stevens (1963), with permission from copyright holder

was possible because no light intensities near the threshold of detectability were included. The data obtained for the light-adapted eyes were fitted by a line obeying Eq. 2.15

$$\psi = k(L - L_o)^{\beta} \tag{2.15}$$

where ψ means the brightness in assigned numbers, k, a dimensional constant, L, light intensity, L_o, the threshold light intensity, and β, an exponent on the order of 0.33. Clearly, the fit is not very good because the line misses 4 out of 6 points. On the other hand, the three lowest points fall on the intermittent line that follows direct proportionality with light intensity, in agreement with the law of asymptotic linearity.

The validity of the law of asymptotic linearity can also be tested by means of a visual experiment of an entirely different kind. It concerns visual estimation of line length. Substantial literature indicates that subjective line length is a power function of physical line length with an exponent approximating unity (e.g. Zwislocki, 1983).

A recent experiment has shown, however, that this is not true for very short, thin lines for which the exponent approaches asymptotically a value of 2 (Sanpetrino, 2005). This power exponent corresponds to the dimension of intensity and is consistent with the law of asymptotic linearity, which does refer to intensity. The experiment was not performed to test the prospective law of asymptotic linearity but, rather, to calibrate individual observers with cochlear implants for loudness measurements. The convergence of the subjective line lengths on the slope of two at very short line lengths was obtained incidentally. Thin lines, 1-mm thick, were projected horizontally on a smooth white wall of a width substantially greater than the longest line used, so that boundary effects were minimized. No marks were present on the wall from which the length of the lines could be inferred. The lines were projected with the help of a power-point set up, and their length was varied practically continuously by means of a digital controller connected to a computer. Both methods, absolute magnitude estimation and absolute magnitude production, were applied. In the first, lines of various lengths were presented 3 times in a random order; in the second, numbers were given within the range previously used by the observers. Like the lines, every number was given 3 times in a random order. The responses associated with the first set of trials for the line lengths or numbers were discarded, the responses associated with the second and third trials were pairwise geometrically averaged. Because of small differences between the magnitude-estimation and production results, both sets have been combined to form a common scatter plot shown by the circles on double-logarithmic coordinates of Fig. 2.19. To bring the trend of the data more clearly in evidence, the scatter plot has been divided into sections along the abscissa axis, and median values of the sections have been determined. They are marked by solid triangles in the figure. Finally, the medians have been approximated by two straight lines according to the least-squares method. The line extending beyond the abscissa of 3 cm has a slope of 0.95, practically 1; the line holding for smaller lengths, a slope of 2.1, practically 2. The corresponding product moment coefficients amount to 0.92 and 0.62, respectively. The modest value of the latter is due to a substantial scatter of the individual data.

Other averaging schemes were attempted, among them, polynomial curve fitting of the entire scatter plot. Although the curve slope depended on the order of the polynomial for very short lines, it remained greater than 1 for all polynomials of orders higher than 1 and hovered around 2 for polynomials between the orders of 2 and 5. In view of this finding and the evidence presented in Fig. 2.19, there can be little doubt that the law of asymptotic linearity holds for apparent length, provided the line is sufficiently thin. Thicker lines cannot be shortened enough for the phenomenon of accelerated apparent shortness to appear. They become thicker than they are long.

Available empirical data allow a test of the law of asymptotic linearity in yet another sense modality, this one concerning the sensation of warmth. The sensation is of particular interest because its threshold lies well above the null of physical heat energy. The situation is somewhat similar to that of partial auditory masking by random noise that can shift the threshold of audibility of a pure tone by a comparable amount. As shown in Fig. 1.4, the slope of the loudness function then

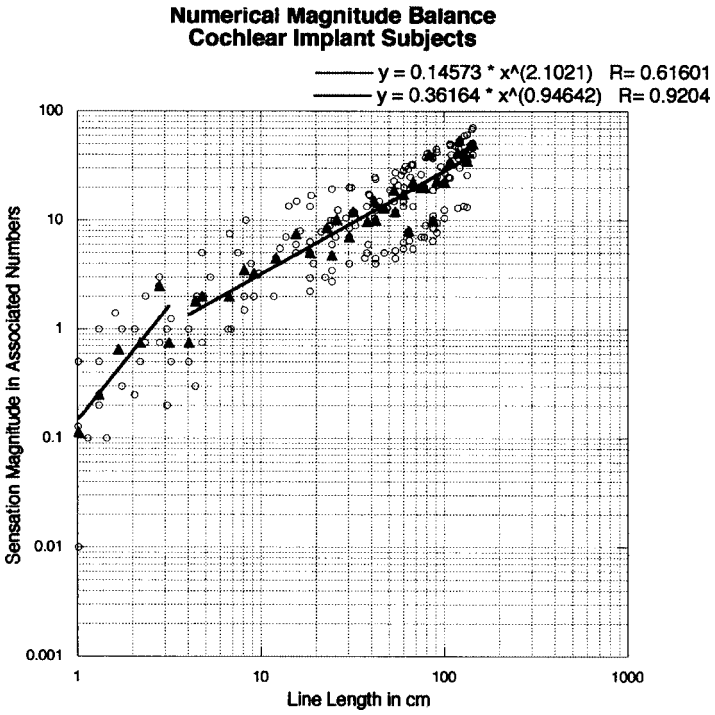

Fig. 2.19 Subjective length of thin lines measured by numerical magnitude balance on six observers as a function of the physical line length. Every observer made three estimates of every length and produced three lengths. The first response was discarded and the remaining two were averaged geometrically. The unfilled circles show the individual geometric means. Because of a small difference between the magnitude estimations and productions, the means have been combined to a common scatterplot. The scatterplot has been divided along the abscissa axis into narrow sections, and medians of the data within the sections have been determined. They are indicated by filled triangles. The medians have been fitted by two straight lines according to the least-squares method, one for the physical lengths smaller than 3 cm, the other, for greater lengths. The slope of the former obeys approximately the square of the physical length, the slope of the latter, the physical length (Sanpetrino-Anzalone, unpublished data, 2005)

becomes steeper than in the absence of the noise and the steepness increases with the threshold shift. One example of the growth of subjective warmth magnitude with heat intensity is shown in Fig. 1.20 (data from J.C. Stevens and Marks, 1971; graph modified from Marks, 1974). The stimulus consisted of a heat flux generated by a 1 kW projection lamp aimed at the forehead. The forehead was painted with India ink to facilitate heat absorption. The variable area of exposure was controlled by aluminum masks, and the exposure time, by a shutter that was opened every 30 s for 3 s. The radiant intensity was measured with a Hardy radiometer. The resulting data shown in Fig. 1.20 are based on magnitude estimates produced by 15 observers relative to reference standards they chose themselves. The heat intensity and the

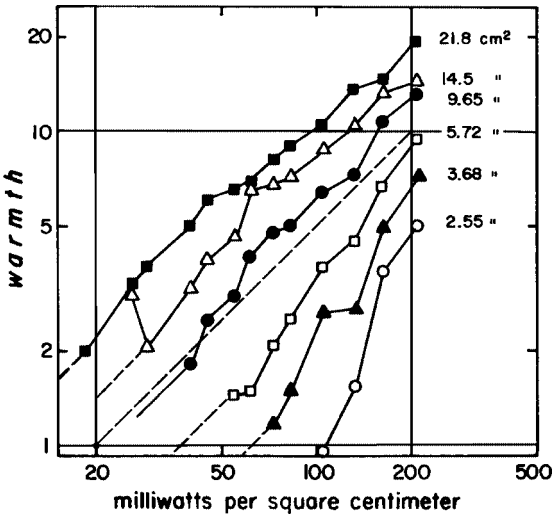

Fig. 2.20 Magnitude of warmth sensation produced by radiant heat on the forehead as a function of heat intensity and irradiated area. The heat was produced by a 1 kW projection lamp, and the forehead was painted with India ink to facilitate heat absorption. The area of exposure was controlled with aluminum masks, and the exposure duration with a shatter that was opened for 3 s every 30 s. A group of 15 observers made magnitude estimates of warmth sensation relative to standards they chose themselves. The heat intensity and the irradiated area were varied at random within the same sequence of presentations. The data points indicate geometric means of the group responses, and the points belonging to the same irradiated area are connected by straight lines. The intermittent lines are their linear extrapolations. Modified from Marks (1974)

irradiated area were varied at random in the same sequence of presentations. The data points indicate that the heat sensation grew with both heat intensity and the exposed area and grew faster with the intensity as the area was decreased. They were originally fitted by a family of smooth curves following the form of Eq. 2.15 and converging at high heat intensities on one point (J.C. Stevens and Marks, 1971). However, this fit was not very satisfactory, and other schemes were attempted, all showing one or another deficiency and running into the fundamental objection of implying a zero sensation at the threshold of detectability. This is only possible on the unrealistic assumption of the absence of internal noise. For these reasons, the data points of Fig. 2.20 have been simply joint by straight lines within each set (Marks, 1974). In addition, intermittent lines have been drawn to extrapolate the sets parallel to the slope of one indicated by the intermittent line that extends between the abscissas of 20 and 200 mW per cm^2. With the exception of one idiosyncratic point, the extrapolating lines seem to be consistent with the point sets and to form a curve pattern similar to that of partial auditory masking in Fig. 2.11, in agreement with the law of asymptotic linearity.

The inference that warmth sensation increases in direct proportion to heat intensity near its threshold of detectability is supported by the finding that the threshold decreases nearly in inverse proportion to exposure duration (Stevens et al., 1973).

This means that the magnitude of warmth sensation is nearly directly proportional to linear temporal summation of heat intensity.

In the preceding examples, the law of asymptotic linearity has been applied to sensory systems responding to physical stimuli, such as mechanical pressure or displacement, light or heat. Does the law apply to chemoreceptive systems of gustation and olfaction? The available experimental data suggest that it does but they are insufficient for a definitive answer. Suprathreshold responses have attracted the main attention and only a few experiments have included near-threshold stimuli. The overall results may be summarized as follows. For clearly suprathreshold stimuli, the subjective magnitudes grow according to power functions of concentrations of the chemical substances. Only a few exceptions are encountered, two prominent ones concerning sucrose (Fig. 1.39) and fructose in gustation (Moskowitz, 1970). Whereas sugars tend to produce power-function exponents for sweetness slightly greater than 1 with a mean of 1.33 (Moskowitz, 1970), acids tend to produce exponents smaller than 1 for sourness (Moskowitz, 1971). In olfaction, all the odorants seem to generate power functions with exponents smaller than unity (Cain and Moskowitz, 1974).

The dichotomy between the exponents greater and smaller than 1 is of interest for the law of asymptotic linearity. For the law to be satisfied, power functions with exponents greater than 1 must become concave upwards near the threshold of detectability, those with exponents smaller than 1, concave downwards. Unfortunately, the scarce near-threshold data reveal these trends only occasionally. They can be seen in Figs. 2.21 and 2.22, the former for the sweetness of six hexose

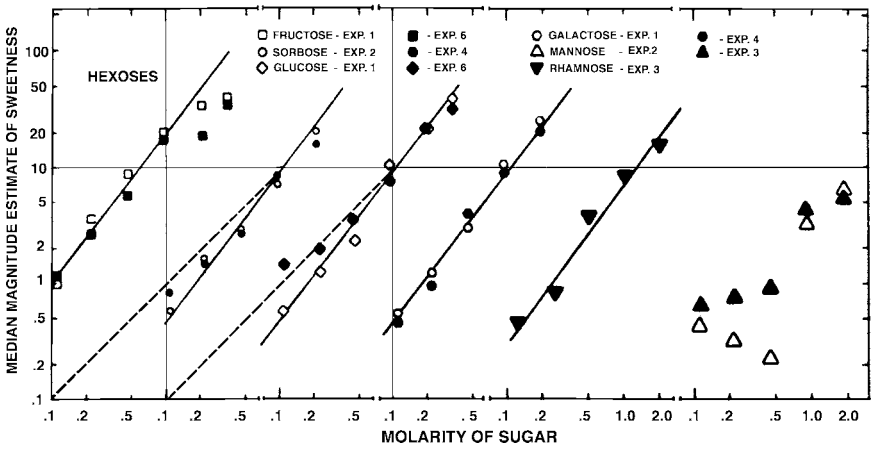

Fig. 2.21 Sweetness magnitudes of several hexose sugars as functions of concentration. The solutions involved were made of reagent-grade chemicals in Cambridge (Mass.) tap water and presented to the observers in paper cups at a temperature of 19°. The sweetness magnitudes were numerically estimated by observers selected from a group of 83 relative to standards they chose themselves. With the exception of rhamnose, the sweetness of every sugar was judged twice. The results are indicated by the various symbols and approximated by power functions (except mannose). The intermittent lines show a linear relationship to the sugar concentration. Modified from Moskowitz (1970), reproduced with permission from the Psychonomic Society

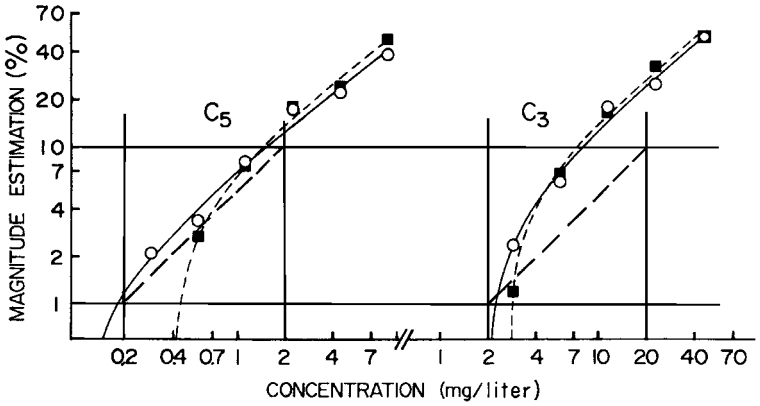

Fig. 2.22 Odorants, *n*-propanol (C_3) and *n*-pentanol (C_5) diluted in odorless air were presented to the observers through two tubes of an olfactometer at a flow rate of 4 l/min for C_3 and 6 l/min for C_5. One tube served for the adapting stimulus, the other, for the test stimulus, both containing the same odorant. The timing of the stimuli was controlled by electromechanical relays. A group of 19 observers made numerical magnitude estimates of odor intensity after adaptation to the same odor, which was achieved by taking three or eight breaths of the diluted odorant. Every observer made two estimates relative to a standard they chose themselves. Subsequently the standards were normalized to the number 10, and the individual responses were geometrically averaged. The data points show the medians of these geometric means, the unfilled circles for the three-breaths adaptation, the filled squares, for the eight-breaths one. The solid and intermittent curves were fitted to the data according to Eq. 2.15. The straight lines indicated by the long-dashes parallel the linear relationship between the subjective odor intensity and odorant concentration. Modified from Cain and Engen (1969), reproduced with permission from the Psychonomic Society

sugars (Moskowitz, 1970), the latter, for the odors of two odorants, *n*-propanol and *n*-pentanol (Cain and Engen, 1969). The data of Fig. 2.21 were obtained by the method of magnitude estimation referred to standards chosen by the observers themselves. The solutions involved were prepared of various quantities of reagent-grade chemicals and Cambridge (Massachusetts) tap water. They were presented to the observers in paper cups containing 5–10 ml of the solution to be sampled at a temperature of 19°. The different concentrations were presented in irregular order, and the observers rinsed their mouths after every presentation. Various subgroups of observers chosen from a total group of 83 participated in the experiments. The subjective sweetness of every sugar, except rhamnose, was measured in two sessions. With the exception of the results for mannose, the obtained data points followed approximately power functions. However, for small concentrations of sorbose and glucose, they partially deviated from such functions upwards, in agreement with the law of asymptotic linearity, as is evident in Fig. 2.21, where the intermittent lines indicate the slope of 1. Similar deviations occurred for some other sugars not included in the figure. That the effect was always small and did not occur in connection with all sugars was probably due to two causes – the exponents of the power functions deviated only modestly from unity, and the data were spars near the thresholds of detectability. Nevertheless, all the deviations from the power functions were consistent with the law of asymptotic linearity.

The olfactory data of Fig. 2.22 were also obtained by means of magnitude estimation relative to the number chosen by each observer for the first stimulus presented. Subsequently, all the individual data were normalized by assigning to the first stimulus the number 10, so that the data do not express absolute values. A group of 19 observers participated in the experiment, and every one of them judged the subjective intensity of every stimulus twice. The data points of Fig. 2.22 indicate the group medians of the geometric means of these pairs of judgments. The stimuli consisted of odorants diluted in odorless air in various proportions and were presented to the observers through two tubes of an olfactometer, one serving for the test odorant the other for an adapting odorant. In Fig. 2.22, both odorants consisted of the same chemicals. The flow rate amounted to 4 l/min for propanol (C_3) and to 6 l/min for pentanol (C_5). The timing of the flow was controlled by electromechanical relays. In the adapting condition, the observers were allowed to take three (unfilled circles) or eight (filled squares) breaths at a rate controlled by a metronome. In the following test condition, they took one breath. At sufficiently high concentrations, the data points followed approximately power functions with exponents smaller than unity; at lower concentrations, the slope of the curves approximated by the data points increased in apparent agreement with the law of asymptotic linearity. The data points were originally approximated, probably incorrectly, by theoretical curves obeying Eq. 2.15 and having a vertical asymptote at vanishingly small concentrations. In fact, the lowest three points for *n*-pentanol (C_5) obtained with weak adaptation (three breaths) are consistent with a slope of 1 indicated by the intermittent line with the longer dashes. Stronger adaptation (eight breaths) increased the slope above 1 within the experimental range of concentrations but the slope at lower concentrations remained unknown. The experiments with *n*-propanol (C_3) produced a similar pattern of results, except that all the slopes implied by the data points were greater. Still, the locations of the lowest two points obtained for weaker adaptation appear to be consistent with a slope of 1 (intermittent line with the long dashes) within the experimental error. Of course, the adaptation probably contributed somewhat to the steepness of the curve implied by the points.

Although the available experimental data on chemoreception do not conclusively support the law of asymptotic linearity, they are not in conflict with it.

A definitive decision will have to await further experimentation.

Multisensory examples of empirical results given above, together with its biophysical basis, suggest that the proposed law of asymptotic linearity may have universal validity in psychophysics. Of course, the universality of an empirical law can never be definitely established and must be continually tested in quest of possible exceptions.

References

Barlow, H.B. Dark and light adaptation: Psychophysics. In: *Handbook of Sensory Physiology VII/4; Visual Psychophysics*, pp. 1–28. D. Jameson and L.M. Hurvich (Eds.), Springer, New York, 1972.

Barlow, R.B., Jr., and Verrillo, R.T. Brightness sensation in a ganzfeld. *Vision Res*. 16: 1291–1297, 1976.

Bolanowski, S.J., and Zwislocki, J.J. Intensity and frequency characteristics of Pacinian corpuscles. I. Action potentials. *J. Neurophys*. 51(4): 793–811, 1984.

Bolanowski, S.J., Gescheider, G.A., Verrillo, R.T., and Checkosky, C.M. Four channels mediate the mechanical aspects of touch. *J. Acoust. Soc. Am*. 84(5): 1680–1694, 1988.

Cain, W.S., and Engen, T. Olfactory adaptation and the scaling of odor intensity. In: *Olfaction and Taste*, pp. 127–141. C. Pfaffmann (Ed.), Rockefeller University Press, New york 1969.

Cain, W.S, and Moskowitz, H.R. Psychophysical scaling of odor. In: *Human Responses to Environmental Odors*, pp. 1–31. Academic Press, New York, 1974.

Feldtkeller, R., Zwicker, E., and Port, E. Lautstärke, Verhältnislautheit und Summenlautheit. *Frequenz* 13: 108–117, 1959.

Fuortes, M.G.F. Generation of responses in receptor. In: *Handbook of Sensory Physiology*, I.W.R. Lowenstein (Ed.), Springer, Berlin-Heidelberg-New York, 1971.

Green, D.M., and Swets, J. *Signal Detection Theory and Psychophysics*. Wiley, New York, 1966.

Hellman, R.P., and Zwislocki, J.J. Some factors affecting the estimation of loudness. *J. Acoust. Soc. Am*. 33: 687–694, 1961.

Hellman, R.P., and Zwislocki, J.J. Monaural loudness function at 1000 cps and interaural summation. *J. Acoust. Soc. Am*. 35: 856–865, 1963.

Hellman, R.P., and Zwislocki, J.J. Loudness sensation of a 1000-cps tone in the presence of a masking noise. *J. Acoust. Soc. Am*. 36: 1618–1627, 1964.

Hellman, R.P., and Zwislocki, J.J. Loudness determination at low sound frequencies. *J. Acoust. Soc. Am*. 43(1): 60–64, 1968.

Kiang, N.Y.-S. A survey of recent developments in the study of auditory physiology. *Trans. Amer. Otol. Soc*. 66: 108–116, 1968.

Marks, L.E. *Sensory Processes: The New Psychophysics*. New York: Academic Press, 1974.

Miller, G.A. Sensitivity to changes in the intensity of white noise and its relation to masking and loudness. *J. Acoust. Soc. Amer*. 19: 609–619, 1947.

Moore, B.C.J. Testing the concept of softness imperception: Loudness near threshold for hearing-impaired ears. *J. Acoust. Soc. Am*. 115(6): 3103–3111, 2004.

Moskowitz, H.R. Ratio scales of sugar sweetness. *Percept. Psychophys*. 7(5): 315–320, 1970.

Moskowitz, H.R. Ratio scales of acid sourness. *Percept. Psychophys*. 9(3B): 371–374, 1971.

Robinson, D.W. The subjective loudness scale. *Acustica* 7: 217–233, 1957.

Sanpetrino, N.M. Unpublished data, 2005.

Scharf, B. Loudness. In: *Handbook of Perception: Vol. 4. Hearing*, pp. 187–242. E.C. Carterette and M.P. Friedman (Eds.), Academic, New York, 1978.

Scharf, B., and Stevens, J.C. The form of the loudness function near threshold. *Proceedings of the 3rd International Congress on Acoustics*, Elsevier, Amsterdam, pp. 80–82, 1961.

Stevens, S.S. The direct estimation of sensory magnitudes-loudness. *Am. J. Psychol*. 69: 1–25, 1956.

Stevens, J.C., and Marks, L.E. Spatial summation and the dynamics of warmth sensation. *Percept. Psychophys*. 9(5): 391–398, 1971.

Stevens, J.C., and Stevens, S.S. Brightness function: Effects of adaptation. *J. Opt. Soc. Am*. 53: 375–385, 1963.

Stevens, J.C., Okulicz, W.C., and Marks, L.E. Temporal summation at the warmth threshold. *Percept. Psychophys*. 14(2): 307–312, 1973.

Teas, D.C., Eldredge, D.H., and Davis, H. Cochlear responses to acoustic transients: An interpretation of whole-nerve action potentials. *J. Acoust. Soc. Am*. 34: 1438–1459, 1962.

Verrillo, R.T. Effects of spatial parameters on the vibrotactile threshold. *J. Exp. Psychol*. 71: 570–574, 1966.

Verrillo, R.T., Fraioli, A., and Smith, R.L. Sensory magnitude of vibrotactile stimuli. *Percept. Psychophys*. 6(A): 366–372, 1969.

Zwicker, E., and Feldtkeller, R. *Das Ohr als Nachrichtenempfanger*. S. Hirzel Verlag, Stuttgart, 1956.

Zwislocki, J.J. Analysis of some auditory characteristics. In: *Handbook of Mathematical Psychology*, Vol. 3, pp. 1–97. R.D. Luce, R.R. Bush, and E. Galanter (Eds.), Wiley, New York, 1965.
Zwislocki, J.J. On intensity characteristics of sensory receptors: A generalized function. *Kybernetik* 12: 169–183, 1973.
Zwislocki, J.J. A power function for sensory receptors. In: *Sensation and Measurements*. H.R. Moskowitz, B. Scharf, and J.C. Stevens (Eds.), Reidel, Dordrecht, Holland, 1974.
Zwislocki, J.J. Group and individual relations between sensation magnitudes and their numerical estimates. *Percept. Psychophys*. 33: 460–468, 1983.
Zwislocki, J.J. Auditory system: Peripheral nonlinearity and central additivity, as revealed in the human stapedius-muscle reflex. *Proc. Nat. Acad. Sci. USA* 99(22): 14601–14606, 2002.
Zwislocki, J.J., and Shepherd, D.C. Unpublished data, 1972.